www.sciencetranslationalmedicine.org/cgi/content/full/5/211/211ra158/DC1

Supplementary Materials for

Sclerostin Inhibition Reverses Skeletal Fragility in an Lrp5-Deficient Mouse Model of OPPG Syndrome

Rajendra Kedlaya, Shreya Veera, Daniel J. Horan, Rachel E. Moss, Ugur M. Ayturk, Christina M. Jacobsen, Margot E. Bowen, Chris Paszty, Matthew L. Warman, Alexander G. Robling*

*Corresponding author. E-mail: arobling@iupui.edu

Published 13 November 2013, *Sci. Transl. Med.* **5**, 211ra158 (2013)
DOI: 10.1126/scitranslmed.3006627

This PDF file includes:

Other Supplementary Material for this manuscript includes the following:
(available at www.sciencetranslationalmedicine.org/cgi/content/full/5/211/211ra158/DC1)

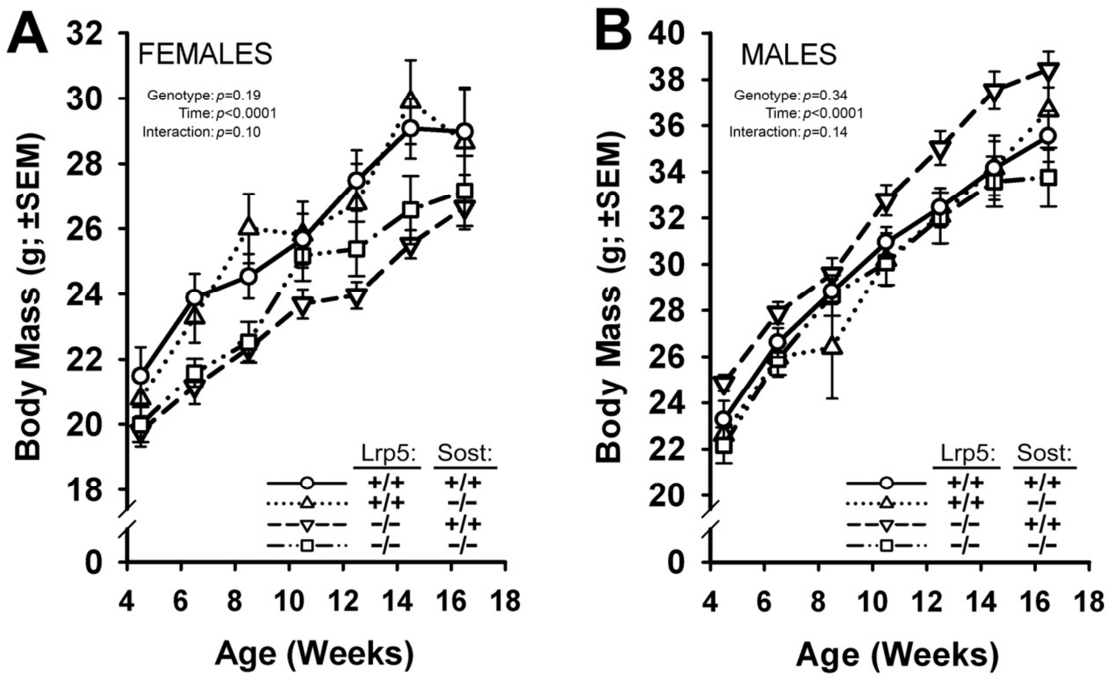

Figure S1: Body mass in mutant Lrp5 and Sost (A) female and (B) male mice. Body weights were collected bi-weekly beginning at 4.5 wks of age until 16.5 weeks of age in wild-type mice (circles; solid line), $Sost^{-/-}$ mice (triangles; dotted line), $Lrp5^{-/-}$ mice (inverted triangles; dashed line), and $Sost^{-/-}$ $Lrp5^{-/-}$ double knockouts (squares; interrupted dashed line). No differences in body mass were detected among groups using repeated measured ANOVA. For each group, *n*=9-14 mice.

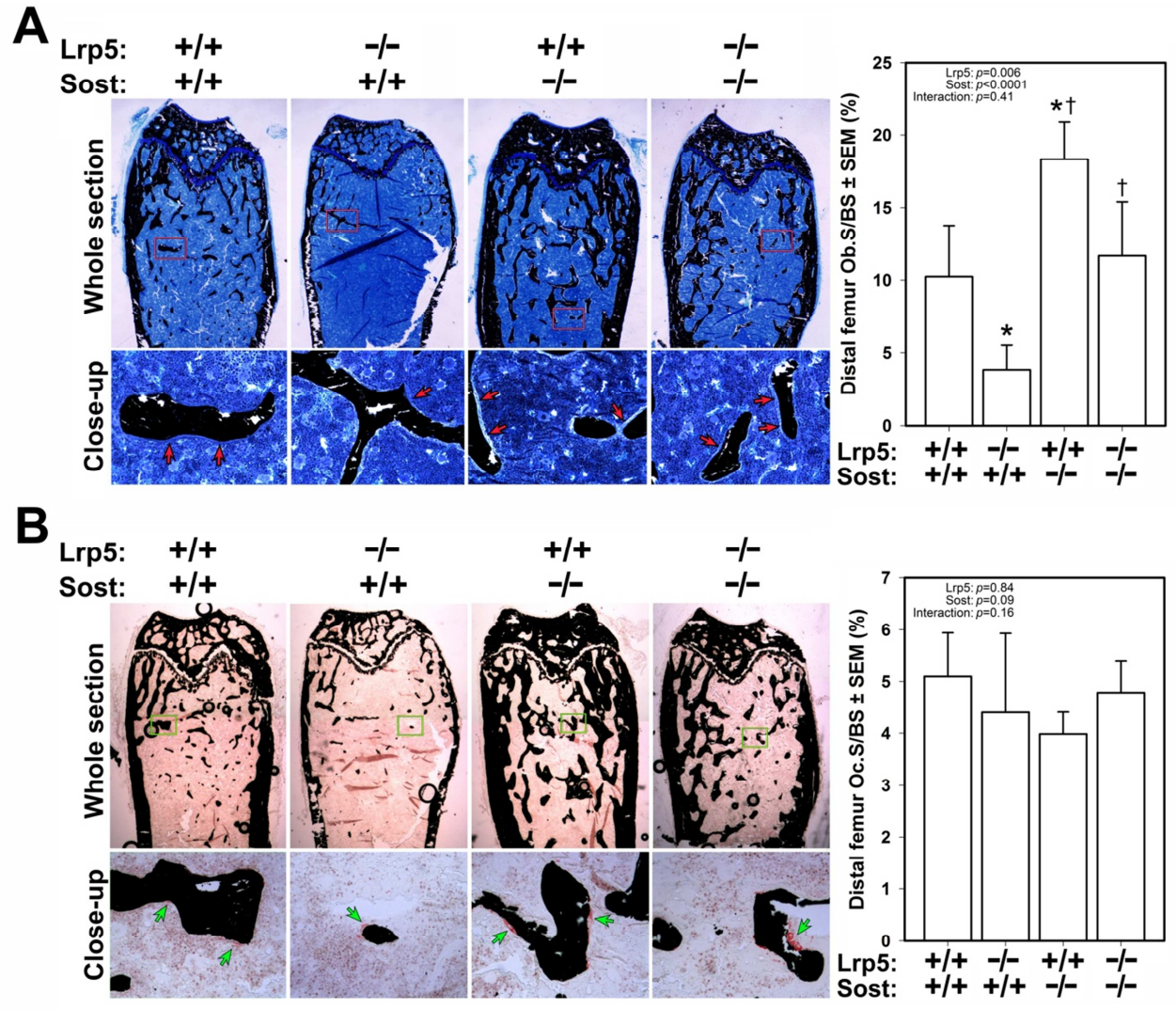

Figure S2: (A) Photomicrographs of MacNeal/von Kossa–stained sections from the distal femur of Sost/Lrp5 mutant male mice. Whole bone (low power) images appear in the upper panels, and higher magnification images of the region contained within the red boxes appear directly below. Red arrows indicate osteoblast-covered surfaces. Osteoblast surface per unit bone surface is indicated in the panel to the right. (B) Photomicrographs of MacNeal/Trap-stained sections from the distal femur of Sost/Lrp5 mutant male mice. Whole bone (low power) images appear in the upper panels, and higher magnification images of the region contained within the green boxes appear directly below. Green arrows indicate osteoclast-covered surfaces. Osteoclast surface per unit bone surface is indicated in the panel to the right. The data were analyzed by 2-way ANOVA within sex using Lrp5 and Sost genotypes as main effects (indicated at the top of each graph). Post-hoc tests were conducted using Fisher's PLSD, and are indicated as follows: * significantly different from WT; † significantly different from $Lrp5^{-/-}$; ‡ significantly different from $Sost^{-/-}$ ($p<0.05$). For each group, n=6 mice.

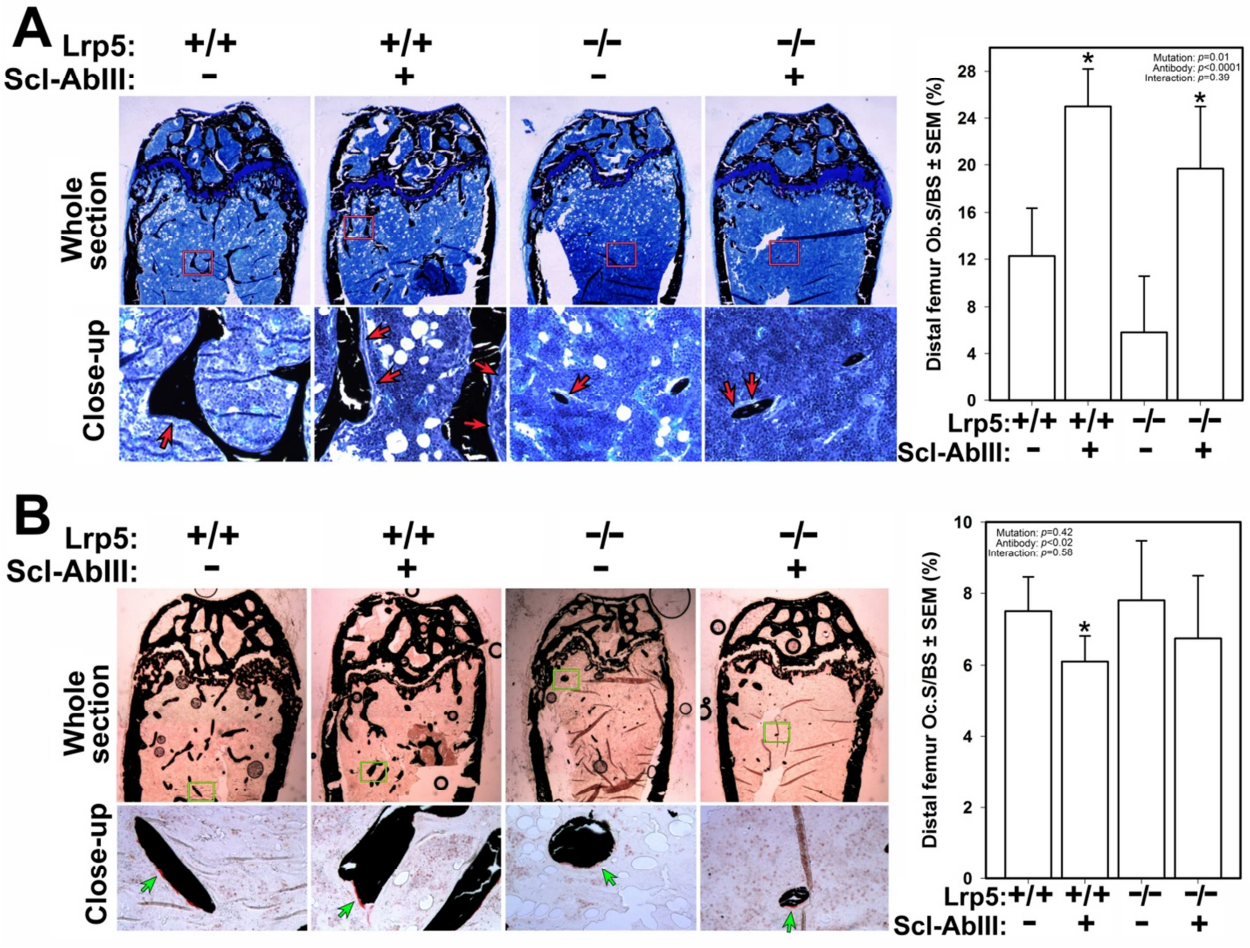

Figure S3: (A) Photomicrographs of MacNeal/von Kossa–stained sections from the distal femur of wild-type and Lrp5$^{-/-}$ mice that were treated for 3 weeks with vehicle (saline) or sclerostin antibody (Scl-AbIII). Whole bone (low power) images appear in the upper panels, and higher magnification images of the region contained within the red boxes appear directly below. Red arrows indicate osteoblast-covered surfaces. Osteoblast surface per unit bone surface is indicated in the panel to the right. (B) Photomicrographs of MacNeal/Trap-stained sections from the distal femur of WT and Lrp5$^{-/-}$ mice that were treated for 3 wks with vehicle (saline) or sclerostin antibody (Scl-AbIII). Whole bone (low power) images appear in the upper panels, and higher magnification images of the region contained within the green boxes appear directly below. Green arrows indicate osteoclast-covered surfaces. Osteoclast surface per unit bone surface is indicated in the panel to the right. The data were analyzed by 2-way ANOVA using Lrp5 genotype and antibody/vehicle treatment as main effects (indicated at the top of both graphs). Post-hoc tests comparing antibody treatment to vehicle treatment within Lrp5 genotypes were conducted using Fisher's PLSD, and a significant difference from vehicle-treated mice is indicated by an asterisk (*; $p<0.05$). For each group, n=6 mice.

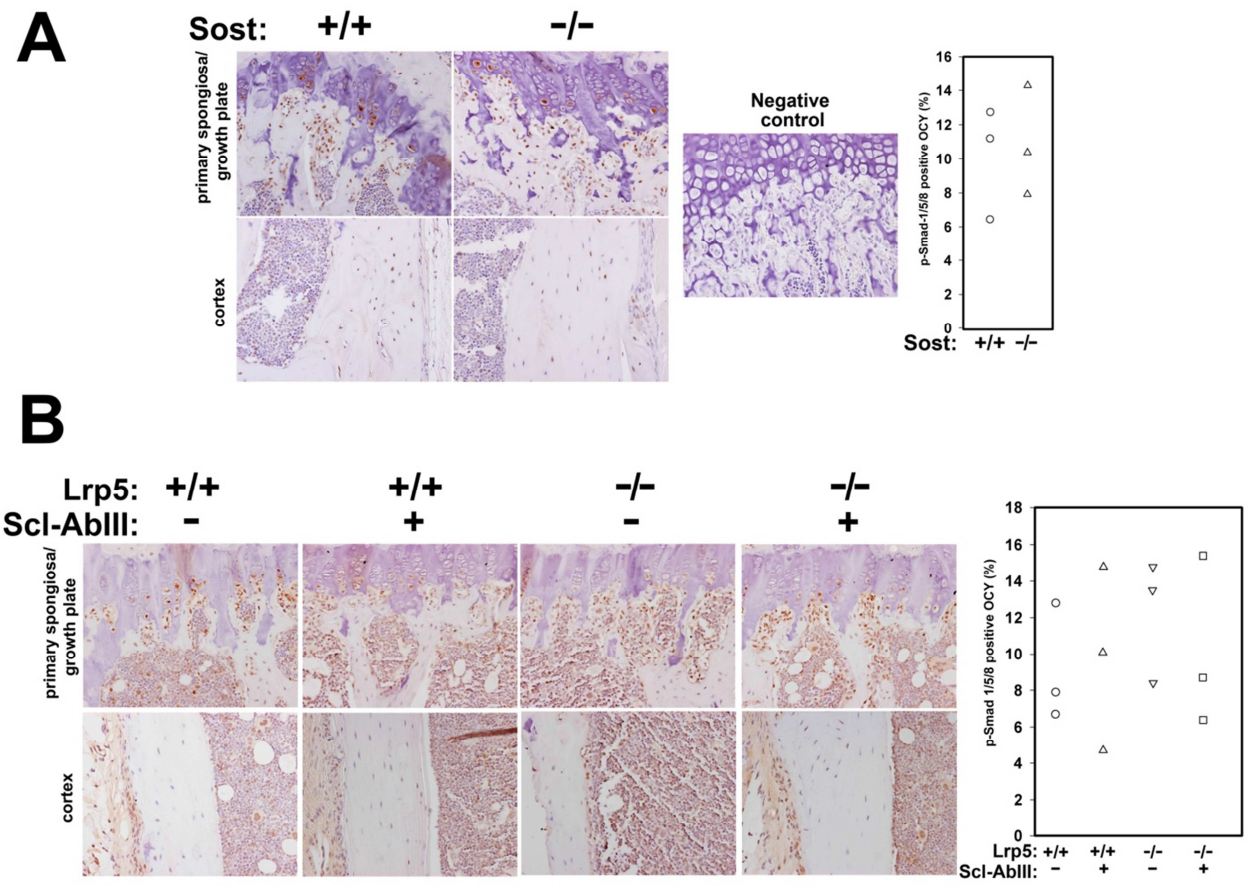

Figure S4: (A) Photomicrographs of the growth plate and primary spongiosa (upper panels) and the cortex (lower panels) from the proximal tibia of 15-week-old wild-type and Sost$^{-/-}$ mice that were immunolabeled for p-Smad 1/5/8 (brown staining) and counterstained with hematoxylin (purple staining). The negative control image is from a WT section that underwent all steps of immunolabeling except for primary antibody incubation. The percent of positively labeled osteocytes from the cortical bone was not different between WT and Sost$^{-/-}$ mice (see scatterplot to the right). Strong p-Smad 1/5/8 staining was detected in the hypertrophic chondrocytes (upper panels) and primary spongiosa, but the cortical osteocytes exhibited very weak labeling. Qualitatively, no obvious differences in staining intensity or localization were noted between genotypes. (B) Photomicrographs of the growth plate and primary spongiosa (upper panels) and the cortex (lower panels) from the proximal tibia of 19-wk-old WT and Lrp5$^{-/-}$ mice that had been treated with vehicle (-) or Scl-AbIII antibody (+). The sections were immunolabeled for phosphorylated Smad 1/5/8 (brown staining) and counterstained with hematoxylin . The percent of positively labeled osteocytes from the cortical bone was not different among WT and Lrp5$^{-/-}$ mice, and Scl-AbIII treatment had no effect on p-Smad within either genotype (see scatterplot to the right). Strong p-Smad 1/5/8 staining was detected in the hypertrophic chondrocytes (upper panels) and primary spongiosa, but the cortical osteocytes exhibited very weak labeling. Qualitatively, no obvious differences in staining intensity or localization were noted between genotypes or treatments.

The data in panel A were analyzed by the Wilcoxon rank-sum test and yielded a nonsignificant outcome (p=0.78). The data in panel B were analyzed by the Kruskall Wallis test and yielded a nonsignificant outcome (p=0.84). For each group, n=3 mice.